Targeted Oncology (2020) 15:377–390
https://doi.org/10.1007/s11523-020-00728-8

ORIGINAL RESEARCH ARTICLE

Co-Regulation of Immune Checkpoint PD-L1 with Interferon-Gamma Signaling is Associated with a Survival Benefit in Renal Cell Cancer

Jörg Hänze[1] · Moritz Wegner[1] · Elfriede Noessner[2] · Rainer Hofmann[1] · Axel Hegele[1]

Published online: 3 June 2020

Abstract

Background Programmed death ligand (PD-L1)-based immune checkpoint blockade therapy for metastatic renal cell carcinoma (RCC) achieves significant response rates in a subgroup of patients. The relevance of PD-L1 gene regulation for disease outcome is not clear**.**

Objective To evaluate PD-L1 expression and its dependence on interferon-γ (IFN-γ) in RCC cell lines and tissues in relation to disease outcome.

Methods and Patients Regulation of *PD-L1*-mRNA and PD-L1 protein was studied in cell lines from clear cell RCC (ccRCC) and papillary RCC (pRCC) by quantitative RT-PCR and Western-blot analysis. *PD-L1*-mRNA correlation and gene-set enrichment analysis (GSEA) of the IFN-γ pathway were conducted with RNA-Seq from ccRCC, pRCC, and skin cutaneous melanoma (SKCM) tissue. In addition, patient overall survival (OS) and disease-free survival (DFS) (cBioPortal for Cancer Genomics) were considered.

Results In ccRCC-like cell lines, PD-L1 was induced by canonical IFN-γ signaling, whereas in a pRCC-like cell line, PD-L1 was refractory towards IFN-γ signaling. In ccRCC and SKCM tissues, GSEA revealed significant IFN-γ pathway activation in tissue samples with high *PD-L1*-mRNA levels. This was not observed in pRCC tissue. ccRCC and SKMC patients with low *PD-L1*-mRNA levels had significantly shorter OS and DFS than those with high *PD-L1*-mRNA levels. In pRCC patients, no significant difference in OS and DFS with regard to *PD-L1*-mRNA tissue levels was obvious.

Conclusions The findings suggest that ccRCC and pRCC differ with respect to PD-L1 regulation by IFN-γ-signaling. High *PD-L1*-mRNA levels in tumor tissues with a positive IFN-γ signature favorably affect OS and DFS.

1 Introduction

Signaling between programmed death (PD-1) and PD-1 ligands (PD-L1 alias CD274; PD-L2 alias CD273 or PDCD1LG2) regulates immune-editing of cancer cells and can be exploited therapeutically as a target for immune checkpoint blockade [1, 2]. Binding between PD-L1 on cancer cells or antigen-presenting cells and PD-1 expressed on T cells elicits co-inhibitory signals. These signals suppress anti-cancer immune responses that involve major histocompatibility complex (MHC) and T-cell receptor (TCR) interactions in the tumor microenvironment [3].

The co-inhibitory signaling pathway can be blocked by intravenous infusion of antibodies against PD-L1 or PD-1 [4]. A considerable percentage of patients in a growing number of malignancies can benefit from this therapy [5]. Renal cell carcinoma (RCC) is resistant to cytotoxic chemotherapy and traditionally less responsive to conventional radiation treatments. In advanced RCC, PD-1/PD-L1-based immune checkpoint blockade therapy was initially approved as second-line monotherapy after anti-angiogenic therapy with tyrosine kinase inhibitors (TKIs). Meanwhile, first-line combination therapies with nivolumab (anti-PD-1 antibody) plus ipilimumab (anti-CTLA-4 antibody), as well as

Electronic supplementary material The online version of this article (https://doi.org/10.1007/s11523-020-00728-8) contains supplementary material, which is available to authorized users.

✉ Jörg Hänze
haenze@staff.uni-marburg.de

[1] Department of Urology and Pediatric Urology, Faculty of Medicine, Philipps-University Marburg, 35043 Baldingerstraße Marburg, Germany

[2] Immunoanalytics Research Group Tissues Control of Immunocytes, Helmholtz Zentrum München, National Research Center for Environmental Health, Munich, Germany

Key Points

Renal cell carcinoma (RCC) cells differ with respect to programmed death ligand (PD-L1) regulation by interferon γ (IFN-γ)-signaling.

In ccRCC cells, intact IFN-γ signaling can induce PD-L1. In pRCC, PD-L1 is refractory towards IFN-γ-pathway signaling.

In tumors with predominantly intact IFN-γ signaling such as ccRCC and melanoma, high *PD-L1*-mRNA levels are associated with prolonged survival of patients; this association is not observed in pRCC patients.

pembrolizumab (anti-PD-1 antibody) or avelumab (anti-PD-L1) each combined with axitinib (TKI) are approved [6–9].

Biomarkers predicting disease outcome and therapy response towards immune checkpoint blockade are highly sought after to avoid treating patients who are unlikely to benefit from this therapy and, thus, will be unnecessarily exposed to immune-related adverse events [10]. Potential markers are PD-L1 expression, infiltration of tumor tissue by immune cells, and tumor mutational burden indicating the abundance of tumor neoantigens [11].

Interferon-γ (IFN-γ) released from immune cells such as T cells, NK cells, and macrophages can induce PD-L1 in adjacent tumor cells via IFN-γ-receptor (IFN-γR) signaling [12]. IFN-γ/IFN-γR signaling triggers tyrosine phosphorylation of Janus kinases (JAK1/2), which targets further downstream signal transducer and activators of transcription (STAT1) and subsequently interferon regulatory factor (IRF1), thereby inducing various target genes, among them PD-L1 and chemokine CXCL10 [13, 14]. IFN-γ has both tumorigenic and immunogenic properties in the tumor microenvironment. In particular, IFN-γ promotes T-cell chemotaxis via the induction of inflammatory chemokines. Conversely, IFN-γ released from T cells attenuates immune responses through induction of *PD-L1*-mRNA/PD-L1 protein on tumor cells. Therefore, we speculate that in tumors such as ccRCC, where PD-Ll is not constitutively driven by oncoviruses (such as EBV), oncogenes (such as ras), or AKT [15], the tissue level of *PD-L1*-mRNA may indicate T-cell responsiveness of these tumors. Since PD-L1 level is under the control of several post-transcriptional mechanisms [16], distinguishing between *PD-L1*-mRNA and PD-L1 protein is critical.

Here, we studied the regulation of *PD-L1*-mRNA and PD-L1 protein by IFN-γ in clear-cell RCC (ccRCC) and papillary RCC (pRCC) cell lines. Additionally, we performed gene expression and IFN-γ-signaling analysis of *PD-L1*-mRNA in tumor tissues with corresponding survival data from patients with ccRCC, pRCC, and skin cutaneous melanoma (SKCM).

2 Material and Methods

2.1 Cell Culture, RNA, and Protein Preparation

Renal cancer cell lines CaKi-1, CaKi-2, Cal-54, and A-498 were cultured in RPMI1640 medium supplemented with 10% fetal bovine serum, 1% stable glutamine, and 1% penicillin/streptomycin solutions (PAA Laboratories, Pasching, Austria) at 37 °C with 5% CO_2 in humidified air [17]. Subconfluent cells were treated with IFN-γ (10 ng/mL from R&D Systems, Minneapolis, MN, USA) for 24 h. RNA extraction was performed with Trifast (Peqlab, Erlangen, Germany) according to the manufacturers' protocol. Protein extraction was performed with RIPA buffer (Cell Signalling Technology Europe, Frankfurt a.M., Germany) supplemented with protease inhibitor cocktail (Sigma-Aldrich Chemie, Munich, Germany) and phosphatase blocker (PhosSTOP, Roche Diagnostics, Mannheim, Germany). Extraction procedure was according to the manufacturers' protocols. The cell lines were from the Leibniz Institute DSMZ-German Collection of Microorganisms and Cell Cultures, Braunschweig, Germany, and were recently authenticated using DNA profiling with highly polymorphic short-tandem repeats (STR) loci. All experiments were performed with tested mycoplasma-free cells (Minerva Biolabs GmbH, Berlin, Germany) and analyses were performed three times.

2.2 Characterization of Renal Cell Carcinoma (RCC) Cell Lines

A recent study explored the genomic similarity of common RCC cell lines and RCC tumor samples including CaKi-1, CaKi-2, A-498, and Cal-54 cell lines [18]. Expression-based classification of ccRCC cell lines assigned CaKi-1 and A-498 cell lines to the aggressive ccRCC subtype and excluded CaKi-2 cell line as ccRCC. Based on further studies, CaKi-2 cell line resembled pRCC, since this cell line harbored typical high-expression levels of MET and LRRK2 [19] as well as chromosome 8 aberrations and MYC activation [20]. Cytological and histologic analysis of CaKi-2 cells in orthotopic and sub-cutaneous mouse models demonstrated typical papillary characteristics [21, 22]. Assignment of Cal-54 cells to either of these subtypes is less certain. The CAL-54 cell line conforms with copy number amplifications (CNAs) in several key kidney cancer genes. CNA-based cluster analysis showed characteristic pRCC alterations [18].

2.3 Quantitative Real-Time RT-PCR

RNA (1 µg) from cell lines was used as a template for cDNA synthesis after digestion of genomic DNA with RNase-free DNase (RevertAid First Strand cDNA synthesis Kit, Fermentas Life Science, St. Leon-Rot, Germany). Real-time RT-PCR was performed with SYBR Green Fluorescein Mix (ABgene UK, Epsom, UK). Cycling conditions were 95 °C for 15 min, followed by 45 cycles of 95 °C for 15 s, 60 °C for 15 s, and 72 °C for 30 s. Relative levels of mRNA are displayed as delta cycle threshold (ΔCt) values (log-2-scale) with the mean of TATA-binding protein (TBP) as reference mRNA. The primer sets were synthesized commercially (Biomers, Ulm, Germany). The gene sequences of forward (+) and reverse primer (−) are listed in Table S1.

2.4 Western Blot

Protein samples (40 µg, determined by Pierce BCA Protein Assay (ThermoFisher, Scientific, Darmstadt, Germany)) were subjected to sodium dodecyl sulphate polyacrylamide gel electrophoresis (gradient gel 4–20%) and transferred to nitrocellulose membranes by electro-blotting (Bio-Rad, Munich, Germany). The membranes were blocked at room temperature for 1.5 h in TRIS-buffered saline with 0.1% Tween containing 5% dry milk, and then the primary antibodies were added and incubated at 4 °C for 24–48 h. The antibodies were as follows: PD-L1 #13684, PD-L2 #82723, STAT1 #9172, JAK1 #3344, phospho-JAK1 #74129, IRF1 #8478, JAK2 #3230, phospho-JAK2 #3771; host rabbit (Cell Signalling Technology Europe, Frankfurt a.M., Germany); β-actin (#MAK6019); host mouse (Linaris, Dossenheim, Germany). Then, secondary antibodies against rabbit (Linaris) or mouse (Thermo Fisher) coupled with horseradish peroxidase were added for band detection with enhanced chemiluminescent luciferase kit (Thermo Scientific, Rockford, IL, USA) by an imager system (Fluorchem IS-8900, Alpha Innotech, San Leandro, CA, USA).

2.5 Patients, Datasets, and Statistical Analysis

The cBioPortal for Cancer Genomics provided gene expression data obtained by RNA-Seq from Kidney Renal Clear Cell Carcinoma (ccRCC; TCGA Provisional), Kidney Renal Papillary Cell Carcinoma (pRCC; TCGA Provisional), and Skin Cutaneous Melanoma (SKCM; TCGA Provisional) with matching clinical patients' data (v2.2.1; https://www.cbioportal.org/) [23, 24]. Co-expression analysis of PD-L1 was performed by online software from cBioPortal (Supplementary Tables S2–S4). Selected *r* values were analyzed by one-way ANOVA with subsequent Dunn's multiple comparisons test (Table 1) employing Graphpad Prism Version 7.04. For survival analysis, data of patients with SKCM, ccRCC, and pRCC were sorted according to median *PD-L1*-mRNA levels employing MS-Office Excel. The comparison of survival curves is indicated by hazard ratios (Mantel–Haenszel) and significant differences were determined by the Log-rank (Mantel-Cox) test. The clinicopathological parameters of patients in relation to *PD-L1*-mRNA levels are given in Tables 2, 3, and 4. Information about the type of therapy includes whether neoadjuvant and adjuvant treatment has been carried out or not. Specific information about systemic therapy was not available. Significant differences of the clinicopathological parameters between low and high *PD-L1*-mRNA level groups were analyzed by the Chi-square test (Tables 2, 3 and 4).

2.6 Gene Set Enrichment Analysis (GSEA)

Analyses of RNA-Seq data of SKCM, ccRCC, and pRCC were conducted with GSEA v4.0.3 for Windows (Joint project of University of California San Diego and Broad Institute: https://www.gsea-msigdb.org/gsea/index.jsp) [25,

Table 1 Ranking of the top PD-L1-mRNA correlates with members related to the IFN-γ pathway in tissues from SKCM, ccRCC, and pRCC

Correlate	SKCM			ccRCC			pRCC		
	r value	rank #	*q* value	*r* value	rank #	*q* value	*r* value	rank #	*q* value
STAT1	0.807	1	1.49E-105	0.466	95	6.64E-28	0.395	861	7.98E-11
IFNG	0.746	8	1.20E-81	0.241	2230	8.07E-08	0.187	4522	3.88E-03
IRF1	0.732	16	3.25E-77	0.263	1880	3.77E-09	0.030	9568	6.92E-01
CXCL10	0.731	17	7.64E-77	0.425	231	4.96E-23	0.366	1173	2.26E-09
JAK2	0.624	255	1.72E-50	0.567	2	4.55E-43	0.439	473	2.63E-13
		Total 20,164			Total 20,180			Total 20,139	

One-way ANOVA (three groups) Kruskal–Wallis test: $p = 0.0009$***

Follow-up: Dunn's multiple comparisons test SKCM vs. ccRCC: $p = 0.071$; SKCM vs. pRCC: $p = 0.007$**; ccRCC vs. pRCC, $p > 0.9999$

r value Spearman value, *q value* multiple corrected significance, *rank* position relative to all correlated RNA-seq genes, total gene number

Table 2 SKCM TCGA patient data: clinicopathological parameters in relation to PD-L1 mRNA level expression

Variable	All cases (*n*)	Low-PD-L1 (*n*)		High PD-L1 (*n*)		*p* value
Age (years)						
< 58	220	106	48.2%	114	51.8%	0.511
≥ 58	240	123	51.3%	117	48.8%	
Sum	460	229		231		
Gender						
Female	175	80	45.7%	95	54.3%	0.172
Male	285	149	52.3%	136	47.7%	
Sum	460	229		231		
Race category						
White	437	214	49%	223	51%	0.287
Non-White	13	9	69.2%	4	30.8%	
NA	10	6	60%	4	40%	
Sum	460	229		231		
Tumor stage						
0	6	3	50%	3	50%	0.081
I	77	33	42.9%	44	57.1%	
II	140	84	60%	56	40%	
III	169	81	47.9%	88	52.1%	
IV	22	10	45.5%	12	54.5%	
NA	46	18	39.1%	28	60.9%	
Sum	460	229		231		
Lymph node						
n0	230	121	52.6%	109	47.4%	0.866
n1	73	33	45.2%	40	54.8%	
n2	49	22	44.9%	27	55.1%	
n3	54	27	50%	27	50%	
Nx	35	17	48.6%	18	51.4%	
NA	19	9	47.4%	10	52.6%	
Sum	460	229		231		
Metastasis						
m0	411	205	49.9%	206	50.1%	0.764
m1	23	10	43.5%	13	56.5%	
NA	26	14	53.8%	12	46.2%	
Sum	460	229		231		
Clark level						
I	5	3	60%	2	40%	0.069
II	18	6	33.3%	12	66.7%	
III	76	32	42.1%	44	57.9%	
IV	167	86	51.5%	81	48.5%	
V	51	34	66.7%	17	33.3%	
NA	143	68	47.6%	75	52.4%	
Sum	460	229		231		
Neoadjuvant treatment						0.523
No	435	215	49.4%	220	50.6%	
Yes	25	14	56%	11	44%	
Sum	460	229		231		
Adjuvant treatment						
No	428	212	49.5%	216	50.5%	0.912
Yes	23	12	52.2%	11	47.8%	
NA	9	5	55.6%	4	44.4%	
Sum	460	229		231		

NA not available

[a]Chi-square test

[b]Median age

Table 3 ccRCC TCGA patient data: clinicopathological parameters in relation to PD-L1 mRNA level

Variable	All cases (*n*)	Low-PD-L1 (*n*)		High PD-L1 (*n*)		*p* value
Age (years)						
< 61	264	126	47.7%	138	52.3%	0.279
≥ 61	269	141	52.4%	128	47.6%	
Sum	533	267		266		
Gender						
Female	188	81	43.1%	107	56.9%	*0.017*
Male	345	186	53.9%	159	46.1%	
Sum	533	267		266		
Race category						
White	462	232	50.2%	230	49.8%	0.508
Non-White	64	33	51.6%	31	48.4%	
NA	7	2	28.6%	5	71.4%	
Sum	533	267		266		
Tumor stage						
I	267	138	51.7%	129	48.3%	0.102
II	57	19	33.3%	38	66.7%	
III	123	66	53.7%	57	46.3%	
IV	83	43	51.8%	40	48.2%	
NA	3	1	33.3%	2	66.7%	
Sum	533	267		266		
Lymph node						
n0	240	111	46.3%	129	53.8%	0.267
n1	16	9	56.3%	7	43.8%	
Nx	277	147	53.1%	130	46.9%	
Sum	533	267		266		
Metastasis						
m0	22	11	50%	11	50%	0.167
m1	3	3	100%	0	0%	
Mx	8	6	75%	2	25%	
NA	500	247	49.4%	253	50.6%	
Sum	533	267		266		
Grading						
g1	14	6	42.9%	8	57.1%	0.706
g2	229	107	46.7%	122	53.3%	
g3	206	110	53.4%	96	46.6%	
g4	76	40	52.6%	36	47.4%	
Gx	5	2	40%	3	60%	
NA	3	2	66.7%	1	33.3%	
Sum	533	267		266		
Neoadjuvant treatment						
No	516	261	50.6%	255	49.4%	0.215
Yes	17	6	35.3%	11	64.7%	
Sum	533	267		266		
Adjuvant treatment						
No	31	20	64.5%	11	35.5%	0.098
NA	502	247	49.2%	255	50.8%	
Sum	533	267		266		

NA not available

[a]Chi-square test

[b]Median age

Table 4 pRCC TCGA patient data: clinicopathological parameters in relation to PD-L1 mRNA level

Variable	All cases (*n*)	Low-PD-L1 (*n*)		High PD-L1 (*n*)		*p* value[a]
Age (years)[b]						
< 61	135	67	49.6%	68	50.4%	0.950
≥ 61	152	76	50%	76	50%	
NA	2					
Sum	287	143		144		
Gender						
Female	76	27	35.5%	49	64.5%	*0.003*
Male	213	118	55.4%	95	44.6%	
Sum	289	145		144		
Race category						
White	206	108	52.4%	98	47.6%	0.130
Non-White	69	28	40.6%	41	59.4%	
NA	14	9	64.3%	5	35.7%	
Sum	289	145		144		
Tumor stage						
I	171	90	52.6%	81	47.4%	0.467
II	21	11	52.4%	10	47.6%	
III	52	21	40.4%	31	59.6%	
IV	15	6	40%	9	60%	
NA	30	17	56.7%	13	43.3%	
Sum	289	145		144		
Lymph node						
n0	50	25	50%	25	50%	0.388
n1	24	8	33.3%	16	66.7%	
n2	4	2	50%	2	50%	
Nx	210	110	52.4%	100	47.6%	
NA	1	0	0%	1	100%	
Sum	289	145		144		
Metastasis						
m0	95	41	43.2%	54	56.8%	0.089
m1	9	2	22.2%	7	77.8%	
Mx	170	94	55.3%	76	44.7%	
NA	15	8	53.3%	7	46.7%	
Sum	289	145		144		
Neoadjuvant treatment						(*)
No	289	145	50.2%	144	49.8%	
Yes	0	0		0		
Sum	289	145		144		
Adjuvant treatment						
No	158	92	58.2%	66	41.8%	
Yes	1	1	100%	0	0%	
NA	130	52	40%	78	60%	(**)
Sum	289	145		144		

NA not available

*Not applicable

**Difference in NA ratio > 2

[a]Chi-square test

[b]Median age

26]. We tested two gene sets by GSEA. The first gene set (*gs-ifng-sig-table1*) corresponds to the five correlates of *PD-L1*-mRNA displayed in Table 1. The second gene set (*geneset-ifng-m14004)* was downloaded from Molecular Signatures Database (MSigDB) v7.1 and comprises 88 genes (Table S5). The statistical values of GSEA are explained in the legend to Fig. 2.

3 Results

3.1 Regulation of PD-L1 in RCC Cells

Initially, we scanned PD-L1, PD-L2, and critical mediators of IFN-γ signaling in two ccRCC cell lines (CaKi-1, A-498), one undefined RCC cell line Cal-54, and one pRCC cell line (CaKi-2). Transcripts of *PD-L1*, *PD-L2*, *IFN-γR1*, *IFN-γR2*, *IRF1*, *STAT1*, *JAK1*, and *JAK2* were detected (Fig. 1a), with the exception of *PD-L2*-mRNA, which was not detectable in CaKi-2 cells. *PD-L1*, *PD-L2, JAK2*, *STAT1*, and *IRF1* mRNAs were induced by IFN-γ in CaKi-1, A498, and Cal-54 cells but not in CaKi-2 cells. Regulation of *PD-L1*-mRNA was congruent with the regulation of *CXCL10*-mRNA, a typical chemokine target gene of IFN-γ.

Concordantly, at the protein level (Fig. 1b) we observed strong PD-L1 induction in CaKi-1, A498, and Cal-54, but not in CaKi-2 cells. PD-L2 was induced by IFN-γ in CaKi-1 and A-498, but not in CaKi-2 and Cal-549 cells. IFN-γ triggered phosphorylation of JAK2 (phospho-JAK2) and JAK1 (phospho-JAK1) as an off–on response in CaKi-1, A-498, and Cal-54 cells. In CaKi-2 cells, phospho-JAK2/JAK1 was not detectable at all. The non-phosphorylated form of JAK1 was unchanged in CaKi-1 and Cal-54 cells, not detectable in CaKi-2 cells, and induced in A-498 cells. The non-phosphorylated form of JAK2 appeared only slightly induced in the IFN-γ-responsive cells. The transcription factor IRF1 was only induced by IFN-γ in IFN-γ-responsive CaKi-1, A-498, and Cal-54 cells, but not in CaKi-2 cells. Critical components of the IFN-γ-signaling cascade are illustrated in Fig. 1c.

3.2 Co-Expression Analysis of PD-L1-mRNA with RNA-Seq Data from SKCM, ccRCC, and pRCC tissues

Next, we performed co-expression analysis of *PD-L1*-mRNA (obtained from RNA-Seq data) against all detectable mRNAs in the RNA-Seq-data sets from ccRCC, pRCC, and SKCM tissues, respectively. Correlates from the IFN-γ-signaling cascade (STAT1, IFN-γ, IRF1, JAK2) including CXCL10 with correlation values ($r > 0.5$) in SKCM tissue are displayed in Table 1. Their correlation values were also determined in ccRCC and pRCC tissue. ANOVA analysis revealed significant differences between SKCM, ccRCC, and pRCC values ($p < 0.01$). A subsequently performed multiple comparison test determined a significant difference between SKCM and pRCC tissues ($p < 0.01$). The r values for JAK1 were lower than 0.5 (SKCM $r = 0.361$, ccRCC $r = 0.242$, and pRCC $r = 0.328$) and are displayed together with the entire correlation data sets in Tables S2–S4.

3.3 Gene-Set Enrichment Analysis (GSEA) for the IFN-γ-Pathway from SKCM, ccRCC, and pRCC Tissues in Relation to High and Low PD-L1-mRNA Levels

Since PD-L1 regulation appeared heterogeneously connected to the IFN-γ pathway in SKCM, ccRCC, and pRCC, we performed gene-set enrichment analysis (GSEA) of the RNA-Seq data sets for the IFN-γ-pathway. The GSEA is a test to determine if a gene set (e.g., derived from the IFN-γ-pathway) may have an association with a biological category (e.g., high and low PD-L1 expression level). Here, we tested two gene sets for the IFN-γ-pathway. The first gene set termed gs-ifng-sig-table1 comprises the five PD-L1-mRNA correlates from Table 1. The second gene set, named gs-ifng-m14004, comprises 88 genes (Supplementary Table S5). The GSEA plots for both gene sets document that the IFN-γ-pathway was activated in cases with high *PD-L1*-mRNA levels in SKCM and ccRCC tissues but not in pRCC tissues. Both gene sets yielded similar results. The more comprehensive gene set (*gs-ifng-m14004*) had the highest enrichment score (ES) in SKCM tissues (ES = 0.825, FDR, q value 0.0; FWER p value 0.0) (Fig. 2a, right panel) followed by ccRCC tissues (ES = 0.542, FDR, q value 0.0603; FWER p value 0.031) (Fig. 2b, right panel). In pRCC tissues, a negative ES value was calculated that did not reach significance (ES = −0.0404, FDR, q value 0.243; FWER p value 0.119) (Fig. 2c, right panel). The corresponding values of gene set *gs-ifng-sig*-table1 were: SKCM tissues (ES = 0.966, FDR, q value 0.008; FWER p value 0.004) (Fig. 2a, left panel) followed by ccRCC tissues (ES = 0.918, FDR, q value 0.0059; FWER p value 0.003) (Fig. 2b, left panel). In pRCC tissues, a negative ES value was calculated that did not reach significance (ES = -0.684, FDR, q value 0.325 FWER p value 0.157) (Fig. 2c, left panel).

3.4 Analogy Between PD-L1-mRNA Regulation in RCC Cell Lines and in RCC Tumor Tissues

The suggested analogy between *PD-L1*-mRNA regulation in RCC cell lines (Fig. 3a) and in RCC tumor tissues (Fig. 3b) is illustrated by correlation graphs of PD-L1 with JAK2, which was selected due to its tightest correlation with IFN-γ signaling in ccRCC (see Table 1). Cells in quadrant Q1 represent those with low *PD-L1*-mRNA levels under basal

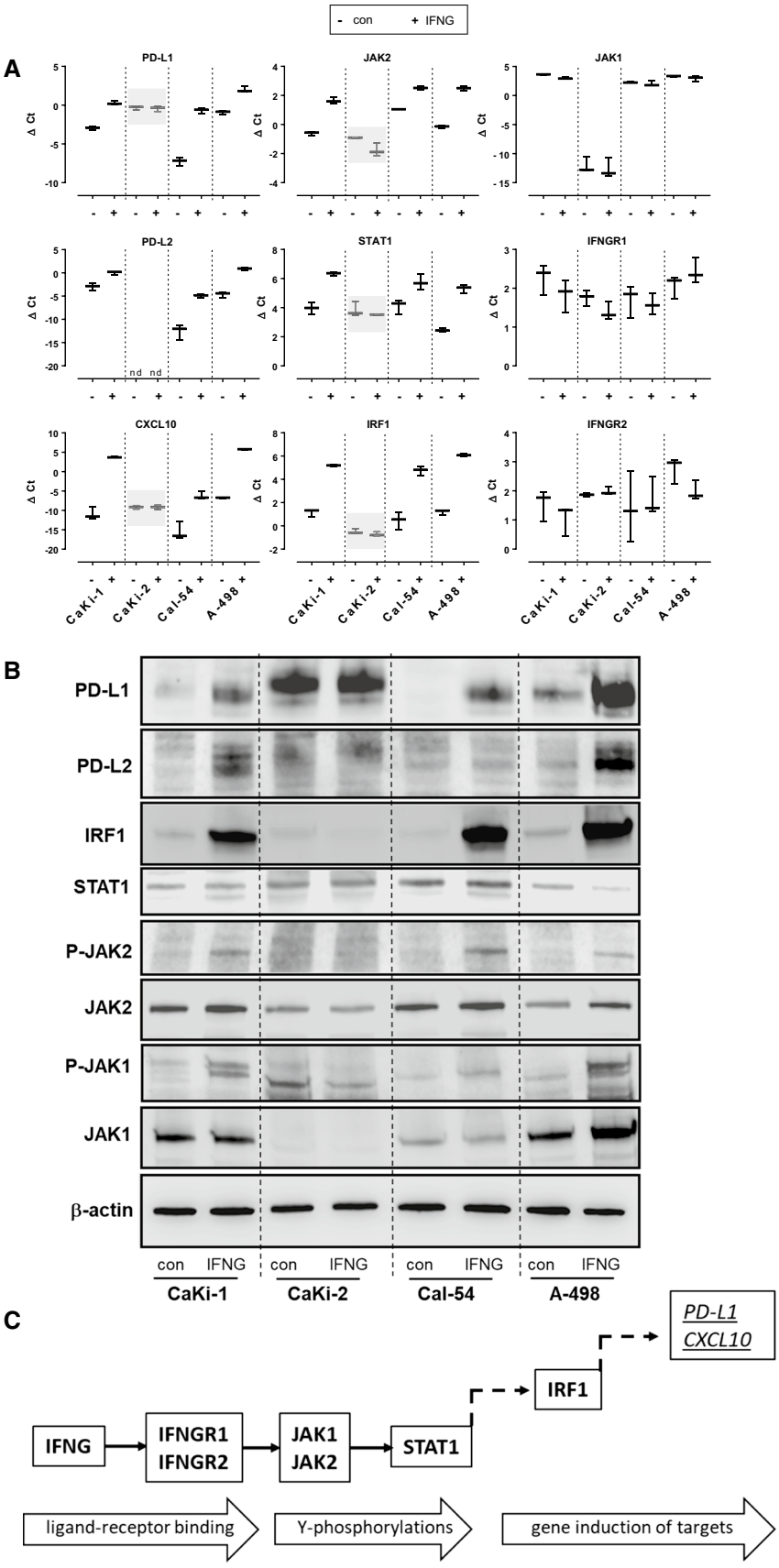

Fig. 1 Regulation of PD-L1 and components of the IFN-γ-signalling cascade in ccRCC cell lines (CaKi-1, A-498), pRCC cell line (CaKi-2) and Cal-54 RCC cell line. **a** Levels of mRNA (ΔCt) for *PD-L1, PD-L2, CXCL10, JAK2, STAT1, IRF1, JAK1, IFN-γR1, IFN-γR2* in control cells (−con) and cells treated with IFN-γ (10 ng/ml) for 24 h (+IFN-γ) are shown. Transcripts that were not inducible by IFN-γ in CaKi-2 cells, in contrast to the other cell lines, are gray-shaded. Box plots indicate means with error bars corresponding to minimum and maximum values ($n=3$). **b** Western-blot analysis of control cells (con) or cells treated with IFN-γ (10 ng/ml) for 24 h with antibodies for PD-L1, p-JAK2, JAK2, p-JAK1, JAK1, IRF1, and cytoplasmic β-actin. The molecular weights are: PD-L1, ~ 50kd; PD-L2, ~ 50 kd; phosphate (P)-JAK2, 125 kd; JAK2, ~ 125 kd; phosphate (P)-JAK1, 130 kd; JAK1, ~ 130 kd; IRF1, ~ 48 kd; STAT1, ~ 90 kd; β-actin, ~ 43kd. **c** Schematic diagram of analyzed components of the IFN-γ-signaling cascade. *nd* below detection level, *IFNG* IFN-γ, *Y* tyrosine residue

conditions without IFN-γ (control: CaKi-1-con, Cal-54-con, A-498-con). Cells in Q3 are those with high *PD-L1* levels that were induced by IFN-γ (CaKi-1-IFN-γ, Cal-54-IFN-γ, A-498-IFN-γ). Cells in Q4 mirror RCC cells with relative high *PD-L1*-mRNA levels independent of IFN-γ (CaKi-2-con and CaKi-2-IFN-γ). The tumor tissues of ccRCC were similarly plotted according to their PD-L1/JAK2 score (Fig. 3b). The observed distribution mirrors that of the cell lines and may be interpreted in analogy to the cell lines, suggesting that in IFN-γ-responsive RCC tissues, *PD-L1/JAK2*-mRNA tissue levels are mainly allocated to either quadrant Q1 or Q3 depending on the IFN-γ abundance in the tumor microenvironment. The virtual arrow with the color gradient from black to red indicates IFN-γ-dependent induction of PD-L1/JAK2 in Q3 (Fig. 3b).

3.5 Analysis of Patient Survival Data in Relation to PD-L1-mRNA Tumor Tissue Levels

Next, we tested whether *PD-L1*-mRNA tissue levels have prognostic value and relate to disease outcome as measured by overall survival (OS) and disease-free survival (DFS) (Fig. 4). Patients were divided according to the median of the tumor tissue levels of *PD-L1*-mRNA from RNA-Seq data in a low (black dotted line) and high PD-L1 group (red, continuous line), respectively. In SKCM with low *PD-L1*-mRNA tissue levels, patient survival was significantly shorter than in those with high-level *PD-L1*-mRNA levels (OS: HR 1.984; $p < 0.0001$ and DFS: HR 1.436; $p = 0.0046$). In ccRCC, similar differences between high and low *PD-L1*-mRNA were observed (OS: HR 1.571; $p = 0.0029$ and DFS: HR 1.751; $p = 0.0019$). In contrast, in pRCC, no differences in OS and DFS in relation to *PD-L1*-mRNA tissue levels were obvious (OS: HR 0.765; $p = 0.374$ and DFS: HR 0.759; $p = 0.326$).

The clinical information of patients with SKCM, ccRCC, and pRCC in relation to low and high *PD-L1*-mRNA groups is listed in Tables 2, 3, and 4). Statistical analyses indicated no significant differences between clinicopathological parameters in the respective cohorts, with the exception of a biased gender distribution in ccRCC and pRCC (in ccRCC: 43.1% female in the low *PD-L1*-mRNA group vs. 56.9% female in the high *PD-L1*-mRNA group; $p < 0.05$; Table 3, and in pRCC: 35.5% female in the low *PD-L1*-mRNA group vs. 64.5% female in the high *PD-L1*-mRNA group; $p < 0.05$; Table 4).

4 Discussion

Here, we demonstrated that RCC subtypes are heterogeneous with regard to IFN-γ signaling and PD-L1 induction. In ccRCC, PD-L1 induction by IFN-γ signaling predominates whereas in pRCC, PD-L1 is apparently non-responsive to IFN-γ signaling. These conclusions are based on cell experiments where PD-L1 was found to be induced by IFN-γ in ccRCC cell lines but not in a pRCC cell line. Further support comes from *PD-L1*-mRNA co-expression analysis and from Gene Set Enrichment analysis (GSEA) performed with RNA-Seq data of tumor tissues. The enrichment score (ES) for IFN-γ-pathway was significantly higher in the high versus the low *PD-L1*-mRNA level group of SKCM tissues. In ccRCC, ES for IFN-γ-pathway was lower but still significant. In pRCC tissue, the ES for IFN-γ-pathway appeared negative without significance. This ranking of *PD-L1* responsiveness towards IFN-γ signaling relates to patient survival when considering low and high *PD-L1*-mRNA tissue levels. In IFN-γ-responsive tumors such as melanoma and ccRCC, patients with high *PD-L1*-mRNA tissue levels had longer OS and DFS than those with low *PD-L1*-mRNA levels. Survival differences between *PD-L1* high and low groups were not detected in pRCC patients. Of note, we did not observe significant differences in the listed clinicopathological parameters in SKCM, ccRCC, and pRCC patients between high- and low-level *PD-L1*-mRNA groups with the exception of gender distribution (Tables 2, 3, 4). Unfortunately, precise information about the kind of systemic adjuvant and neoadjuvant treatments and, particularly, about immune therapy was not available, which represents a limitation of the present study.

Patient-individual differences in IFN-γ responsiveness may causally translate to the observed differences in patient survival dependent on *PD-L1*-mRNA levels. High *PD-L1*-mRNA levels in IFN-γ-responsive tumor cells may indicate an IFN-γ-dependent inflammatory status of the tumor environment that may be less aggressive, reflected in the observed correlation in longer survival. In particular, T cells release IFN-γ upon pMHC recognition in the context of tumor antigen presentation, subsequently raising the *PD-L1*-mRNA transiently from a basal to a high level in IFN-γ-responsive tumor tissues. Thus, high *PD-L1*-mRNA levels may reflect an acute anti-tumor T-cell attack. Therefore, we suggest the *PD-L1*-mRNA tumor tissue level to be a favorable prognostic marker for those tumors that do not constitutively express PD-L1.

Similarly, in bladder cancer, high *PD-L1*-mRNA tissue levels were associated with longer survival in patients who received neither anti-PD-L1 nor anti-PD-1 therapy [27]. Particularly, high *PD-L1*-mRNA levels were associated with immune cell infiltration potentially reflecting T-cell recognition of tumor cells with IFN-γ secretion in an inflamed tumor microenvironment [27]. In breast cancer, high *PD-L1*-mRNA levels were associated with response to chemotherapy and high *PD-L1*-mRNA tissue levels have been suggested as a marker for anti-tumor immune response [28, 29]. Melanoma patients who were non-responsive towards

SKCM

A

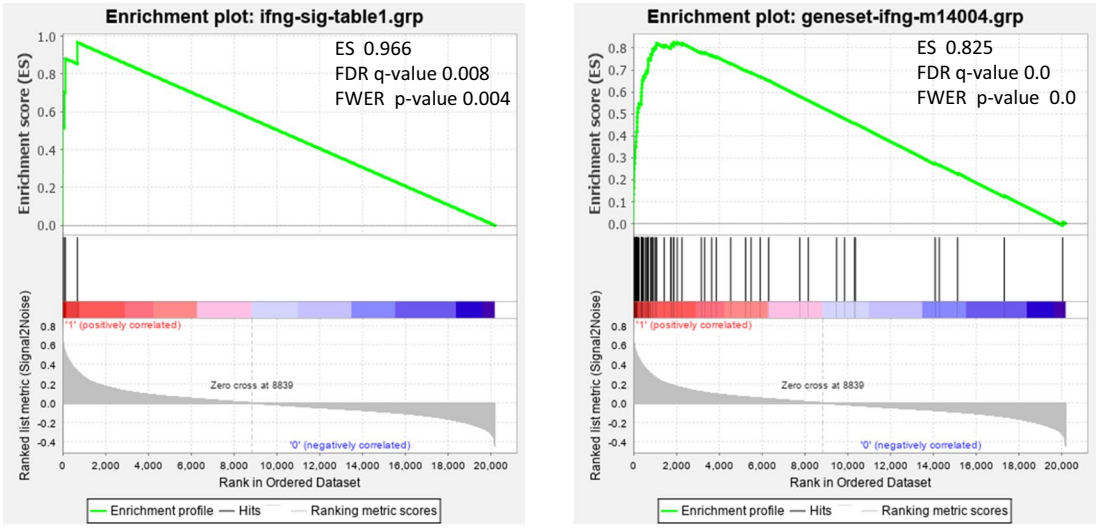

ccRCC

B

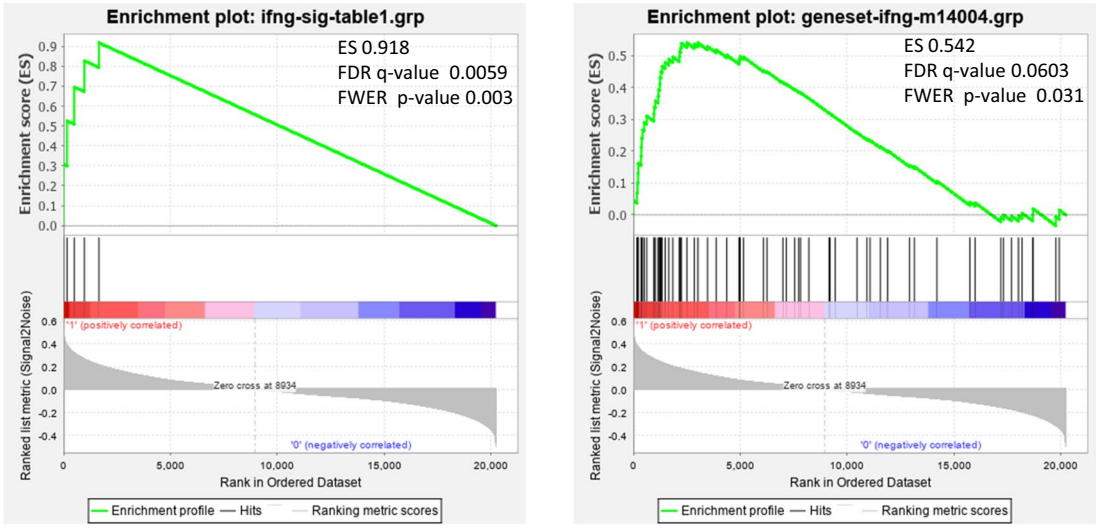

pRCC

C

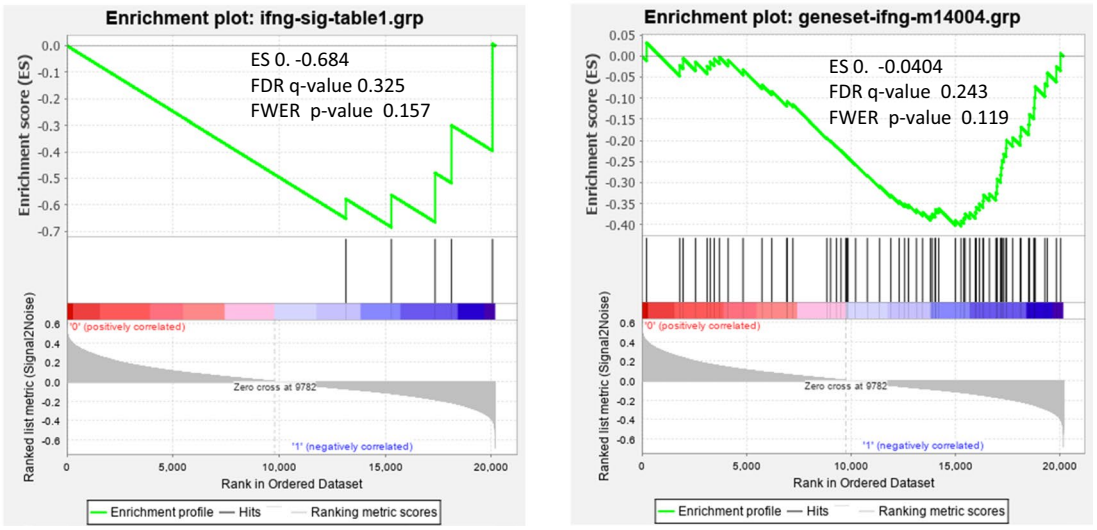

◂**Fig. 2** Gene set enrichment analysis (GSEA) for the IFN-γ pathway in SKCM (**A**), ccRCC (**B**), and pRCC (**C**) tissues. Two gene sets (gs) indicating IFN-γ-signaling were tested. Left panels: *gs-ifng-sig*-table1 with five genes from Table 1. Right panels: *gs-ifng-m14004* with 88 genes from MSigDB. See also description in Sects. 2, and 3, Results. GSEA was performed between dichotomized high- and low-*PD-L1* mRNA level groups based on the respective medians. The enrichment score (ES) was calculated according to the original GSEA statistics [26]. Significances are based on the false-discovery rate (FDR < 25%) and indicated by FDR (*q* value) and familywise-error rate (FWER) *p* values in the insets of the GSEA plots

immune checkpoint therapy targeting CTLA-4 displayed defective IFN-γ signaling [30]. Along this line, loss of function mutations in JAK1/JAK2 that prevent IFN-γ signaling were associated with primary [31] and acquired resistance [32] towards PD-1/PD-L1-based immune checkpoint blockade therapy. Conversely, tandem amplification of PD-L1/PD-L2 and JAK2, causing enhanced IFN-γ signaling, was associated with high responsiveness towards immune checkpoint blockade in Hodgkin's lymphoma [33, 34].

Based on immunohistological detection, PD-L1 protein expression has been investigated as a predictive or prognostic biomarker in various malignancies [35]. The results from these studies differed from the associations of *PD-L1*-mRNA tissue homogenate levels with disease outcome: Contrary to high *PD-L1*-mRNA levels, a high PD-L1 immune histology score was associated with short survival in different malignancies, including RCC, independent of therapy [36]. In melanoma, a high PD-L1 protein score was associated with shorter survival [37]. In particular, a high PD-L1 score, considering PD-L1 in cancer cells or macrophages, predicted both worse outcome and, in a mouse model, the knockout of PD-L1 or of IFN-γ signaling by STAT1-knockdown in tumor cells prolonged survival [37]. Furthermore, in RCC, a high PD-L1 protein score was predictive of poor outcome in patients who received anti-angiogenic TKI treatment with sunitinib or pazopanib (COMPARZ trial) [38]. In contrast, patients with tumors that displayed a high T-effector gene signature score, correlating with a high PD-L1 protein level in immune cells within RCC tumor tissues, were suggested

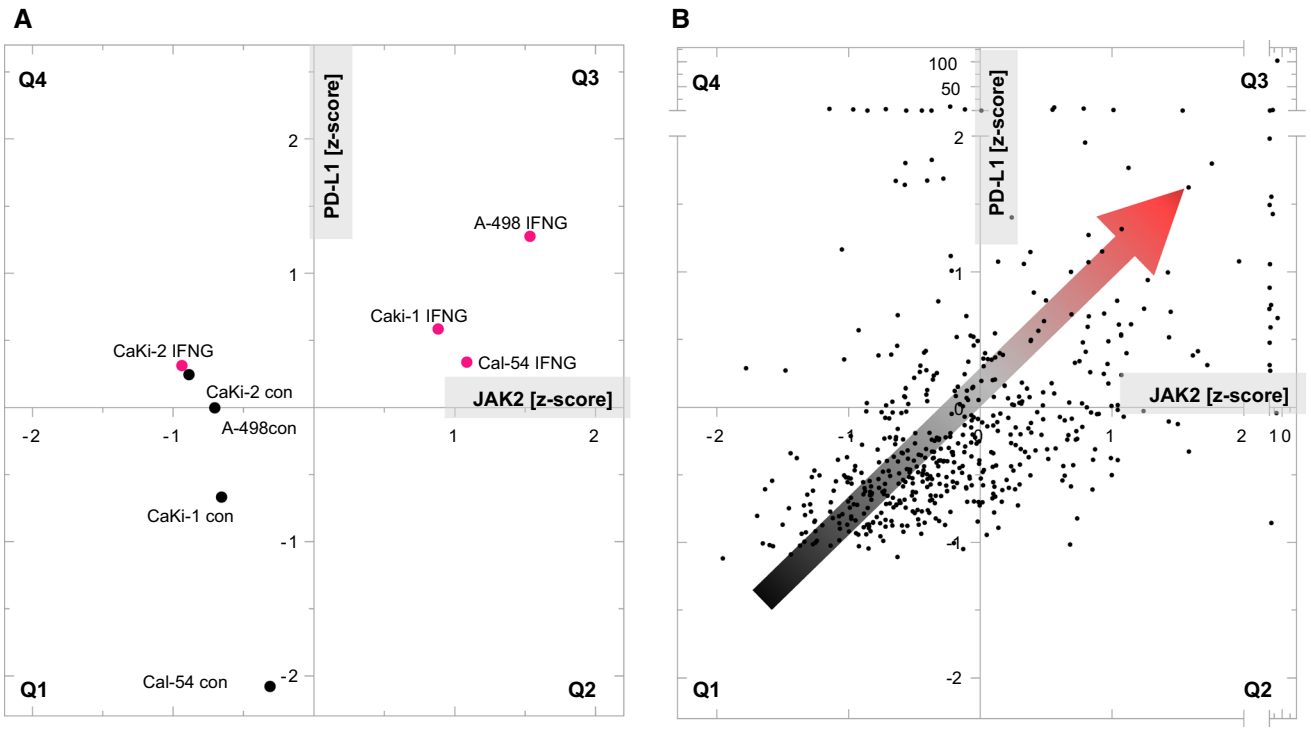

Fig. 3 Correlation graph of *PD-L1*-mRNA (y-axes) and *JAK2*-mRNA (x-axes) in RCC cell lines (**a**) and ccRCC tissues (**b**). The samples (z-score values) are allocated in quadrants (Q1–Q4). **a** Q1 reflects IFN-γ-responsive cells (CaKi-1, A-498, Cal-54) under basal culture conditions without IFN-γ (cell name with extension con, black dots), Q3 the same cells after IFN-γ induction (red dots). Q4 contains the pRCC cell line CaKi-2 that is non-responsive to IFN-γ [CaKi-2 control (black) and IFN-γ-treated cells (red)]. **b** Allocation of *PD-L1/JAK2* mRNA levels detected in ccRCC tumor tissues. The positioning of the tissues (each represented by a dot) in the quadrants may be similarly interpreted to cell lines. The virtual arrow with the color gradient from black to red suggests IFN-γ-dependent induction of *PD-L1/JAK2-mRNA* in Q3. A perfect positive correlation ($r = 1$) would allocate the dots exclusively on the arrow (crossing Q1 to Q3). In case of less ($r < 1$) or no correlation ($r = 0$) the dots deviate from the arrow and become distributed over all quadrants (see Table 1 for the *r* values of SKCM, ccRCC, and pRCC between *PD-L1-mRNA* with JAK2-mRNA)

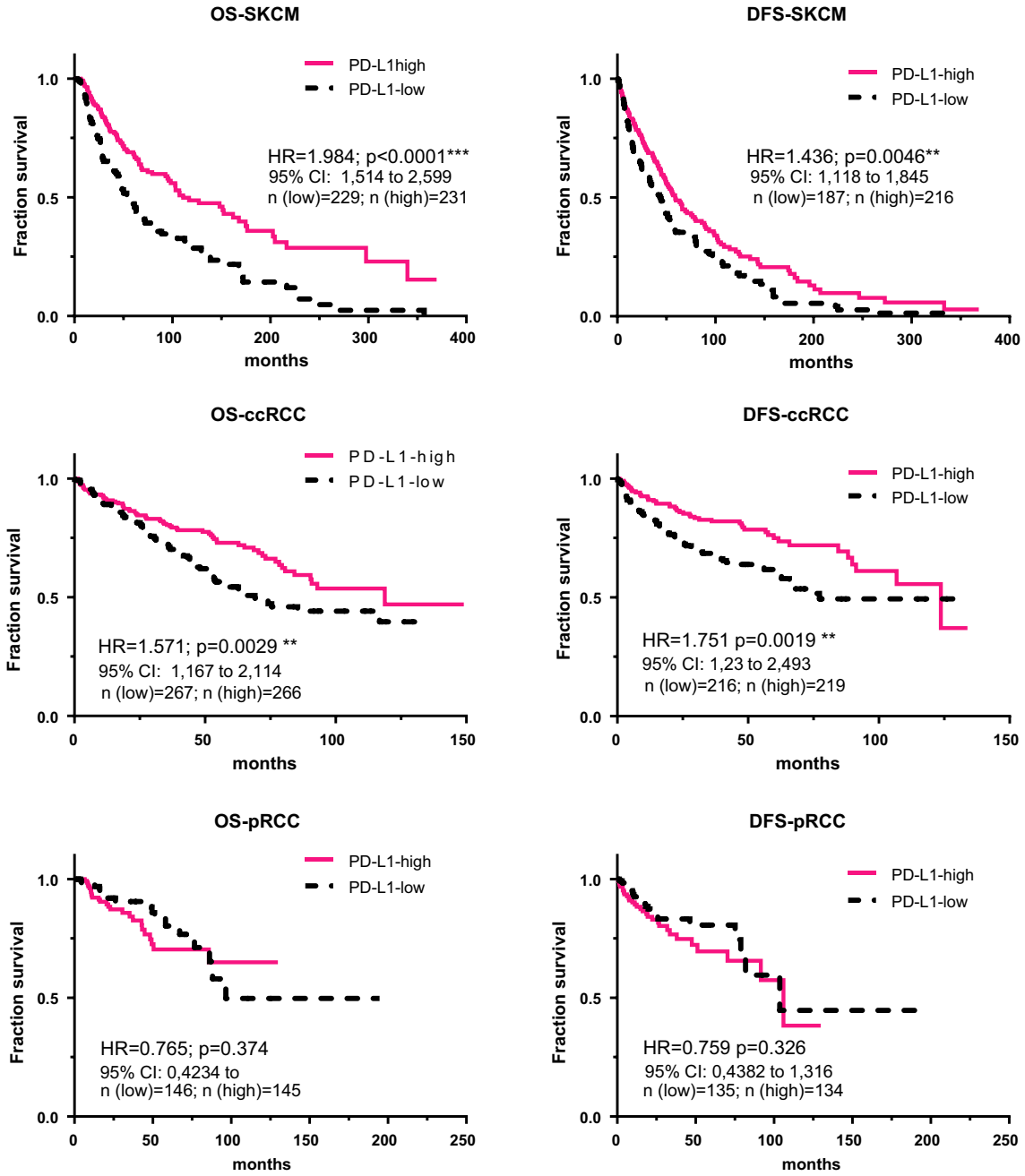

Fig. 4 Kaplan–Meier survival curves of overall survival (OS) and disease-free survival (DFS) from patients with SKCM, ccRCC, and pRCC. Patients were divided according to the median of the tumor tissue levels of PD-L1-mRNA from RNA-Seq data in a low- (black dotted line) and high-PD-L1 group (red, continuous line), respectively. Hazard ratio (HR), *p* value (*p*), and the number of patients are indicated. All available RNA seq data and survival data were considered. However, the number of RNA seq data was higher than those of patients' survival and therefore the number within groups can differ

to benefit from combined anti-PD-L1 and antiangiogenic therapy [36].

The contrary associations between patient survival and PD-L1 immunoscore (high PD-L1 protein/short survival) versus *PD-L1*-mRNA (low *PD-L1*-mRNA/short survival) may seem implausible. However, protein levels and mRNA levels may not be concordant since numerous post-transcriptional regulation mechanisms exist that have relevance for PD-L1. These include signaling proteins such as PBRM1, CMTM4, CMTM6, Ras, MEK, and ERK, which regulate PD-L1 post-transcriptionally [15, 16, 39]. In addition, micro-RNAs may contribute to the regulation. In particular, mir-155 and mir-513 represent targets of IFN-γ signaling with critical impact on PD-L1 mRNA and protein

levels [40–42]. Due to the considerable post-transcriptional influence on PD-L1 protein, the *PD-L1*-mRNA level may more closely reflect the PD-L1 induction that occurs as a consequence of active tumor recognition by T cells. Nonetheless, mRNA detection of tissue homogenates has the limitation that it is not possible to discriminate between expression by cancer cells, immune cells, or other cells of the tissue environment. Therefore, histologic RNA detection by in situ hybridization combined with immune histology in order to identify the cellular context may be a technical advance to improving our understanding of the PD-L1/PD-1 biology in tumor environments and its relation to patient outcome and therapy response. Prospectively, GSEA performed with gene sets for certain cell types and signaling pathways may retrieve deeper information about the tissue biology from RNA-data sets.

Independent of the detection method, it is the interconnected biology of PD-L1 and T-cell activity, the latter measured as IFN-γ response, which indicates the immune-reactive state of the tissue. This can be identified as a correlation of PD-L1 (protein or mRNA) with IFN-γ signaling, or as a spatial co-positioning of PD-L1 protein with T cells in tumor tissues by immune histology. If such a scenario is observed, there is strong evidence of IFN-γ-regulated PD-L1 likely through immune recognition of the tumor cells, which might be reflected in longer survival.

5 Conclusions

In summary, we demonstrated that RCC cells differ with respect to PD-L1 regulation by IFN-γ-signaling. In ccRCC cells, IFN-γ signaling is predominantly intact with IFN-γ-dependent PD-L1 induction. In pRCC, IFN-γ responsiveness is attenuated with PD-L1 expression independent of IFN-γ. In IFN-γ-responsive tumors such as ccRCC and SKCM, high *PD-L1*-mRNA levels are associated with prolonged survival of patients, but not in pRCC patients. We suggest that *PD-L1*-mRNA tumor tissue level correlated to IFN-γ signaling as a marker of favorable prognosis and response to PD-1/PD-1 checkpoint blockade for those tumors that do not constitutively express PD-L1.

Acknowledgements Open Access funding provided by Projekt DEAL. We thank Susanne Lingelbach for excellent technical assistance.

Compliance with Ethical Standards

Funding No external funding was used in the preparation of this article.

Conflict of interest The authors Jörg Hänze, Moritz Wegner, Elfriede Noessner, Rainer Hofmann, and Axel Hegele declare that they have no conflicts of interest that might be relevant to the contents of this article.

References

1. O'Donnell JS, Teng MWL, Smyth MJ. Cancer immunoediting and resistance to T cell-based immunotherapy. Nat Rev Clin Oncol. 2019;16(3):151–67. https://doi.org/10.1038/s41571-018-0142-8.
2. Mittal D, Gubin MM, Schreiber RD, et al. New insights into cancer immunoediting and its three component phases—elimination, equilibrium and escape. Curr Opin Immunol. 2014;27:16–25. https://doi.org/10.1016/j.coi.2014.01.004.
3. Escors D, Gato-Cañas M, Zuazo M, et al. The intracellular signalosome of PD-L1 in cancer cells. Signal Transduct Target Ther. 2018;3:26. https://doi.org/10.1038/s41392-018-0022-9.
4. Grywalska E, Pasiarski M, Góźdź S, et al. Immune-checkpoint inhibitors for combating T-cell dysfunction in cancer. Onco Targets Ther. 2018;11:6505–24. https://doi.org/10.2147/OTT.S150817.
5. Homet Moreno B, Ribas A. Anti-programmed cell death protein-1/ligand-1 therapy in different cancers. Br J Cancer. 2015;112(9):1421–7. https://doi.org/10.1038/bjc.2015.124.
6. Rini BI, Plimack ER, Stus V, et al. Pembrolizumab plus axitinib versus sunitinib for advanced renal-cell carcinoma. N Engl J Med. 2019;380(12):1116–27. https://doi.org/10.1056/NEJMoa1816714.
7. Motzer RJ, Tannir NM, McDermott DF, et al. Nivolumab plus ipilimumab versus sunitinib in advanced renal-cell carcinoma. N Engl J Med. 2018;378(14):1277–90. https://doi.org/10.1056/NEJMoa1712126.
8. Albiges L, Powles T, Staehler M, et al. Updated European association of urology guidelines on renal cell carcinoma: immune checkpoint inhibition is the new backbone in first-line treatment of metastatic clear-cell renal cell carcinoma. Eur Urol. 2019;76(2):151–6. https://doi.org/10.1016/j.eururo.2019.05.022.
9. Motzer RJ, Penkov K, Haanen J, et al. Avelumab plus axitinib versus sunitinib for advanced renal-cell carcinoma. N Engl J Med. 2019;380(12):1103–15. https://doi.org/10.1056/NEJMoa1816047.
10. Šmahel M. PD-1/PD-L1 blockade therapy for tumors with downregulated MHC class I expression. Int J Mol Sci. 2017;18(6):1331. https://doi.org/10.3390/ijms18061331.
11. Miao D, Margolis CA, Gao W, et al. Genomic correlates of response to immune checkpoint therapies in clear cell renal cell carcinoma. Science. 2018;359(6377):801–6. https://doi.org/10.1126/science.aan5951.
12. Garcia-Diaz A, Shin DS, Moreno BH, et al. Interferon receptor signaling pathways regulating PD-L1 and PD-L2 expression. Cell Rep. 2017;19(6):1189–201. https://doi.org/10.1016/j.celrep.2017.04.031.
13. Sallusto F, Lenig D, Mackay CR, et al. Flexible programs of chemokine receptor expression on human polarized T helper 1 and 2 lymphocytes. J Exp Med. 1998;187(6):875–83. https://doi.org/10.1084/jem.187.6.875.

14. Luster AD, Unkeless JC, Ravetch JV. Gamma-interferon transcriptionally regulates an early-response gene containing homology to platelet proteins. Nature. 1985;315(6021):672–6. https://doi.org/10.1038/315672a0.
15. Coelho MA, de Carné Trécesson S, Rana S, et al. Oncogenic RAS signaling promotes tumor immunoresistance by stabilizing PD-L1 mRNA. Immunity. 2017;47(6):1083–1099.e6. https://doi.org/10.1016/j.immuni.2017.11.016.
16. Glodde N, Hölzel M. RAS and PD-L1: a masters' liaison in cancer immune evasion. Immunity. 2017;47(6):1007–9. https://doi.org/10.1016/j.immuni.2017.12.001.
17. Brodaczewska KK, Szczylik C, Fiedorowicz M, et al. Choosing the right cell line for renal cell cancer research. Mol Cancer. 2016;15(1):83. https://doi.org/10.1186/s12943-016-0565-8.
18. Sinha R, Winer AG, Chevinsky M, et al. Analysis of renal cancer cell lines from two major resources enables genomics-guided cell line selection. Nat Commun. 2017;8:15165. https://doi.org/10.1038/ncomms15165.
19. Looyenga BD, Furge KA, Dykema KJ, et al. Chromosomal amplification of leucine-rich repeat kinase-2 (LRRK2) is required for oncogenic MET signaling in papillary renal and thyroid carcinomas. Proc Natl Acad Sci USA. 2011;108(4):1439–44. https://doi.org/10.1073/pnas.1012500108.
20. Furge KA, Chen J, Koeman J, et al. Detection of DNA copy number changes and oncogenic signaling abnormalities from gene expression data reveals MYC activation in high-grade papillary renal cell carcinoma. Cancer Res. 2007;67(7):3171–6. https://doi.org/10.1158/0008-5472.CAN-06-4571.
21. Pulkkanen KJ, Parkkinen JJ, Laukkanen JM, et al. HSV-tk gene therapy for human renal cell carcinoma in nude mice. Cancer Gene Ther. 2001;8(7):529–36. https://doi.org/10.1038/sj.cgt.7700342.
22. Pulkkanen KJ, Parkkinen JJ, Kettunen MI, et al. Characterization of a new animal model for human renal cell carcinoma. Vivo. 2000;14(3):393–400.
23. Gao J, Aksoy BA, Dogrusoz U, et al. Integrative analysis of complex cancer genomics and clinical profiles using the cBioPortal. Sci Signal. 2013. https://doi.org/10.1126/scisignal.2004088.
24. Cerami E, Gao J, Dogrusoz U, et al. The cBio cancer genomics portal: an open platform for exploring multidimensional cancer genomics data. Cancer Discov. 2012;2(5):401–4. https://doi.org/10.1158/2159-8290.CD-12-0095.
25. Mootha VK, Lindgren CM, Eriksson K-F, et al. PGC-1alpha-responsive genes involved in oxidative phosphorylation are coordinately downregulated in human diabetes. Nat Genet. 2003;34(3):267–73. https://doi.org/10.1038/ng1180.
26. Subramanian A, Tamayo P, Mootha VK, et al. Gene set enrichment analysis: a knowledge-based approach for interpreting genome-wide expression profiles. Proc Natl Acad Sci USA. 2005;102(43):15545–50. https://doi.org/10.1073/pnas.0506580102.
27. Breyer J, Wirtz RM, Otto W, et al. High PDL1 mRNA expression predicts better survival of stage pT1 non-muscle-invasive bladder cancer (NMIBC) patients. Cancer Immunol Immunother. 2018;67(3):403–12. https://doi.org/10.1007/s00262-017-2093-9.
28. Denkert C, von Minckwitz G, Brase JC, et al. Tumor-infiltrating lymphocytes and response to neoadjuvant chemotherapy with or without carboplatin in human epidermal growth factor receptor 2-positive and triple-negative primary breast cancers. J Clin Oncol. 2015;33(9):983–91. https://doi.org/10.1200/JCO.2014.58.1967.
29. Bertucci F, Finetti P, Colpaert C, et al. PDL1 expression in inflammatory breast cancer is frequent and predicts for the pathological response to chemotherapy. Oncotarget. 2015;6(15):13506–19. https://doi.org/10.18632/oncotarget.3642.
30. Gao J, Shi LZ, Zhao H, et al. Loss of IFN-γ pathway genes in tumor cells as a mechanism of resistance to anti-CTLA-4 therapy. Cell. 2016;167(2):397–404.e9. https://doi.org/10.1016/j.cell.2016.08.069.
31. Shin DS, Zaretsky JM, Escuin-Ordinas H, et al. Primary resistance to PD-1 blockade mediated by JAK1/2 mutations. Cancer Discov. 2017;7(2):188–201. https://doi.org/10.1158/2159-8290.CD-16-1223.
32. Zaretsky JM, Garcia-Diaz A, Shin DS, et al. Mutations associated with acquired resistance to PD-1 blockade in melanoma. N Engl J Med. 2016;375(9):819–29. https://doi.org/10.1056/NEJMoa1604958.
33. Ansell SM, Lesokhin AM, Borrello I, et al. PD-1 blockade with nivolumab in relapsed or refractory Hodgkin's lymphoma. N Engl J Med. 2015;372(4):311–9. https://doi.org/10.1056/NEJMoa1411087.
34. Sharma P, Hu-Lieskovan S, Wargo JA, et al. Primary, adaptive, and acquired resistance to cancer immunotherapy. Cell. 2017;168(4):707–23. https://doi.org/10.1016/j.cell.2017.01.017.
35. Teng MWL, Ngiow SF, Ribas A, et al. Classifying cancers based on T-cell infiltration and PD-L1. Cancer Res. 2015;75(11):2139–45. https://doi.org/10.1158/0008-5472.CAN-15-0255.
36. McDermott DF, Huseni MA, Atkins MB, et al. Clinical activity and molecular correlates of response to atezolizumab alone or in combination with bevacizumab versus sunitinib in renal cell carcinoma. Nat Med. 2018;24(6):749–57. https://doi.org/10.1038/s41591-018-0053-3.
37. Benci JL, Xu B, Qiu Y, et al. Tumor interferon signaling regulates a multigenic resistance program to immune checkpoint blockade. Cell. 2016;167(6):1540–1554.e12. https://doi.org/10.1016/j.cell.2016.11.022.
38. Choueiri TK, Figueroa DJ, Fay AP, et al. Correlation of PD-L1 tumor expression and treatment outcomes in patients with renal cell carcinoma receiving sunitinib or pazopanib: results from COMPARZ, a randomized controlled trial. Clin Cancer Res. 2015;21(5):1071–7. https://doi.org/10.1158/1078-0432.CCR-14-1993.
39. Burr ML, Sparbier CE, Chan Y-C, et al. CMTM6 maintains the expression of PD-L1 and regulates anti-tumour immunity. Nature. 2017;549(7670):101–5. https://doi.org/10.1038/nature23643.
40. Yee D, Shah KM, Coles MC, et al. MicroRNA-155 induction via TNF-α and IFN-γ suppresses expression of programmed death ligand-1 (PD-L1) in human primary cells. J Biol Chem. 2017;292(50):20683–93. https://doi.org/10.1074/jbc.M117.809053.
41. Gong A-Y, Zhou R, Hu G, et al. MicroRNA-513 regulates B7–H1 translation and is involved in IFN-gamma-induced B7–H1 expression in cholangiocytes. J Immunol. 2009;182(3):1325–33. https://doi.org/10.4049/jimmunol.182.3.1325.
42. Ding L, Lu S, Li Y. Regulation of PD-1/PD-L1 pathway in cancer by noncoding RNAs. Pathol Oncol Res. 2020;26:651–63. https://doi.org/10.1007/s12253-019-00735-9.